SIMULATION OF THE GROWTH OF A $\mathrm{TlInS_2} < \mathrm{Yb} >$ SINGLE CRYSTAL, DFT CALCULATION OF ELECTRONIC PROPERTIES, AND AC CONDUCTIVITY OF SAMPLES

S.M. ASADOV[1], S.N. MUSTAFAEVA[2], S.S. HUSEYNOVA[2]
[1]Azerbaijan State Oil and Industry University, SRI GPOGC. Azerbaijan, Baku
[2]Institute of Physics, Ministry of Science and Education Azerbaijan. Baku
E-mail: solmust@gmail.com

The simulation of the process of growing $\mathrm{TlInS_2}$ and $\mathrm{TlInS_2} < \mathrm{Yb} >$, which has a layered monoclinic syngony with the space group $2/c - C_{2h}^6$, has been carried out. On geometrically optimized $\mathrm{TlInS_2}$ and $\mathrm{TlInS_2} < \mathrm{Yb} >$ supercells, the electronic properties are calculated using density functional theory (DFT). Conductivity was studied in single-crystal samples in alternating electric fields (ac-conductivity – σ_{ac}) across the layers in the frequency range $f = 5 \times 10^4$–3.5×10^7 Hz. In the frequency range $f = 5 \times 10^4$–2.4×10^7 Hz, the ac conductivity of the $\mathrm{TlInS_2} < 1\ \mathrm{at.\%\ Yb} >$ single crystal obeyed the regularity $\sigma_{\mathrm{ac}} \sim f^{0.8}$. The density and energy spread of states lying near the Fermi level, the average time and distance of hops, and the concentration of traps responsible for the conductivity of $\mathrm{TlInS_2} < 1\ \mathrm{at.\%\ Yb} >$ are estimated.

Keywords: Simulation of crystal growth, DFT calculation, Yb-doped $\mathrm{TlInS_2}$ supercell, electronic structure, $\mathrm{TlInS_2}$ and $\mathrm{TlInS_2} < 1\ \mathrm{at.\%\ Yb} >$ single crystal, ac-conductivity.
PACS: 61.72.-y; 71.20.Nr; 72.20.-i

1. INTRODUCTION

The $\mathrm{TlInS_2}$ compound belongs to the $\mathrm{A^{III}B^{III}C_2^6}$ (A = Tl, B = Ga, In, and C = S, Se, Te) family of semiconductor ternary compounds. These crystalline materials have semiconductor and ferroelectric properties and can be used as an active medium for photodetectors in the visible and mid-IR ranges [1]. The crystal structure of the $\mathrm{TlInS_2}$compound is characterized by the formation of various polymorphic modifications: monoclinic [2, 3], orthorhombic [2], tetragonal [4], hexagonal [5], and triclinic systems [6]. The $\mathrm{TlInS_2}$ compound with a monoclinic syngony has a layered structure and is characterized by anisotropy of physical properties. The properties of $\mathrm{TlInS_2}$ crystals are strongly affected, in particular, by the atoms of alloying elements [7]. One of the alloying elements for semiconductors are lanthanides [8].

The purpose of this work is to simulate growth, DFT calculation of the electronic structure, and study the conductivity of $\mathrm{TlInS_2}$ and $\mathrm{TlInS_2} < 1\ \mathrm{at.\%\ Yb} >$ samples in alternating electric fields of the radio frequency range at 298 K.

2. TECHNIQUE OF CALCULATION AND EXPERIMENT

Modeling of temperature fields. The temperature fields and the shape of the crystallization front were studied by computer simulation as a function of the growth rate of $\mathrm{TlInS_2}$ and $\mathrm{TlInS_2} < 1\ \mathrm{at.\%\ Yb} >$. The quality of the grown crystals depends on the composition of the melt and heat and mass transfer in the "crystal-melt" system. The simulation also took into account the crystal growth rate and the size of the growing crystal. The concentration of impurities in our case is small, and they do not affect the temperature fields and the distribution of impurities during directional crystallization of $\mathrm{TlInS_2}$ and $\mathrm{TlInS_2} < 1\ \mathrm{at.\%\ Yb} >$. Modeling of temperature fields in the "crystal-melt" system was carried out by a program based on a two-dimensional model. It was assumed that in a growing crystal the state of the system is in equilibrium at each moment of time. It was assumed that the system has axial symmetry and the growth values depend on the axial coordinate z and on the radius r in the plane perpendicular to the axis. When calculating the temperature field in a growing crystal, heat transfer by the crystal, thermal radiation from the surface of the melt and crystal, and radiation exchange between the crystal and melt were taken into account. The motion of the melt was described within the framework of a viscous incompressible liquid by the Navier-Stokes equation.

DFT electronic structure calculation. The band structure and density of electronic states $\mathrm{TlInS_2}$ with monoclinic syngony (space group $C2/c - C_{2h}^6$) were calculated based on the density functional theory (DFT) using the ATK quantum chemical package [7]. The electronic configurations of atoms in the ground state were considered: Tl – [Xe] $4f^{14}5d^{10}6s^26p^1$, In – [Kr] $4d^{10}5s^25p^1$, S – $3s^23p^4$, Yb – [Xe] $4f^{14}6s^2$. The effects of exchange and correlation into the total energy of the system were taken into account within the framework of the generalized gradient approximation (GGA) according to the Perdew–Burke–Ernzerhof (PBE) scheme [9, 10]. The unit cell geometry $\mathrm{TlInS_2}$ and $\mathrm{TlInS_2} < \mathrm{Yb} >$ was optimized.

The basis was built using plane waves with a kinetic energy ≤ 300 eV. The convergence in total energy in unit cell calculations was no worse than 5×10^{-6} eV/atom. The convergence threshold for interatomic forces was 10^{-4} eV/Å. The choice of k-points of the reciprocal lattice was performed using

131, H.Javid ave, AZ-1143, Baku
Institute of Physics
E-mail: jophphysics@gmail.com

the Monkhorst–Pack method [11]. To subdivide the Brillouin zone of a supercell, a 2 × 2 × 2 k-grid was used [7].

Sample preparation. The synthesis of polycrystals of the compound $TlInS_2$ and $TlInS_2 < 1$ at.% Yb > was carried out using the extremely pure chemical elements Tl (Tl 00), In (In00), S (high purity 16-5) and Yb (99.99%). The completion of the synthesis of $TlInS_2$ and $TlInS_2 < 1$ at.% Yb >, their homogeneity and individuality were controlled by differential thermal (DTA) and X-ray phase (XRD) analysis. DTA was carried out on a STA 449 F3 Jupiter setup. XRD of powder samples was carried out on a D8-ADVANCE diffractometer in the mode 0.5° < 2θ < 80° (Cu Kα radiation; λ = 1.5418 Å) at 40 kV and 40 mA.

Growing single crystals. Heat and mass transfer was simulated during the growth of single crystals. A melt based on $TlInS_2$ in a quartz ampoule was considered a Newtonian fluid in the Boussinesq approximation in the buoyancy term. Melt density is calculated as a linear function of temperature. Taking into account the corresponding hydrodynamic differential equations, the transport fields of the flow, temperature, and dopant Yb and $TlInS_2$ concentrations were calculated. The CGSim program (Crystal Growth Simulator) based on the finite volume method [12] was used for calculations.

Single crystals were grown by the Bridgman-Stockbarger method [13] from synthesized $TlInS_2$ and $TlInS_2 < 1$ at.% Yb > polycrystals. The single crystal growth rate was 0.1 mm/h. A sample in an ampoule placed in the hot zone of the furnace was melted, and the melt was kept at 1050 K for 1–2 h. The grown $TlInS_2$ and $TlInS_2 < 1$ at.% Yb > single crystals had a monoclinic syngony with a space group (sp. gr.) $C2/c - C_{2h}^6$.

The frequency-dependent ac-conductivity of samples of $TlInS_2$ and $TlInS_2 < 1$ at.% Yb > single crystals was measured by the resonance method using a B486 Q-meter [14]. The frequency range of the alternating electric field was 5×10^4–3.5×10^7 Hz. For measurements, $TlInS_2$ and $TlInS_2 < 1$ at.% Yb > samples were prepared in the form of flat capacitors, the plane of which was perpendicular to the crystallographic c-axis of the $TlInS_2$ crystal with a monoclinic system. Silver paste was used as electrodes for samples. The thickness of the samples was 200 μm, and the area of the plates was 4×10^{-2} cm^2. When measuring samples $TlInS_2$ and $TlInS_2 < 1$ at.% Yb >, the reproducibility of the resonance position was ±0.2 pF in capacitance and ±1.0–1.5 divisions of the resonator scale in terms of quality factor ($Q = 1/\mathrm{tg}\delta$). In this case, the largest deviations from the average values were 3–4% for permittivity (ε') of samples and 7% for tgδ [14].

3. RESULTS AND DISCUSSION

Let us consider a mathematical model of the melt motion as a viscous incompressible fluid, which is described by the Navier-Stokes equation

$$\rho v_i(\partial v_i/\partial x_i) - \rho g_i + \rho g_i \alpha_L (T - T_0) - \partial \tau_{ij}/\partial x_j \qquad (1)$$

where ρ is the density of the melt at a given temperature T_0, v_i is the velocity of the fluid element, g_i is the free fall acceleration, α_L is the thermal expansion coefficient, τ_{ij}j is the stress tensor $\tau\tau_{ij} = -p\delta_{ij} + \eta(\partial v_i/\partial x_i + \partial v_j/\partial x_i)$, p is the pressure, η is the viscosity coefficient.

Equation (1) is used with the continuity equations

$$\partial v_i/\partial x_i = 0 \qquad (2)$$

$$\rho c_p v_i \partial T/\partial x_i + \partial q_j/\partial x_i = 0 \qquad (3)$$

where c_p is the heat capacity, $q_j = -k\partial T/\partial x_i$ is the heat flux, k is the thermal conductivity coefficient. The indices i, j take the values of the coordinates, y, z, g_i and v_i the projections of the directions of gravity and velocity on the corresponding coordinates $x_x \equiv x, x_y \equiv y,. x_z \equiv z$. Velocity v_i or force $\tau_{ij}n_j$ on the surface bounding the melt is determined taking into account the normal n_j to the surface: $\tau_{ij}n_j = P_0 n_i$ (P_0 is the gas pressure on the melt surface).

At the “melt–crystal” boundary, the isotherm is determined by $T(r,z) = T_m$ (T_m is the melting temperature). Taking this into account, we write the equation for the heat flux from the melt in the form

$$k_L \nabla T_L n = n(T_L - T_C) + \varepsilon\sigma(T_L^4 - T_r^4) \qquad (4)$$

T_L– melt temperature, T_C – ambient temperature, ε – emissivity, $\sigma = 5.67 \cdot 10^{-8}$ J / (s·m^2· K^4) – Stefan–Boltzmann constant, T_r– effective ambient temperature.

The state of the resulting crystal is determined by the temperature from the heat conduction equation: $\nabla(k_S \nabla T) - \rho_S c_{pS} v_p \nabla T = 0$. The temperature field in the crystal was solved by the method of finite differences of nonlinear equations with partial derivatives [15]. The perfection of a crystal depends on the shape of the crystallization front. The temperature fields in the “crystal–melt” system during crystal preparation were modeled taking into account the crystal diameter and growth rate (0.1–10 mm/h; d = 5–10 mm) (Fig. 1).

It has been established that a proportional change in the diameter of 5-10 mm of the $TlInS_2 < 1$ ат.% Yb > crystal and maintaining a growth rate of 0.1-0.5 mm/h does not change the shape of the crystallization front. The results of modeling the growth of a $TlInS_2 < 1$ ат.% Yb > single crystal with a length of 10–100 mm show that the concentration of the alloying component along the crystal-melt interface is also determined by the competition of convection and diffusion mechanisms. With an increase in the concentration of the alloying component (>1 at.% Yb), the crystallization rate of the melt decreases, and the quality of the crystal depends on the movement of the heat flux.

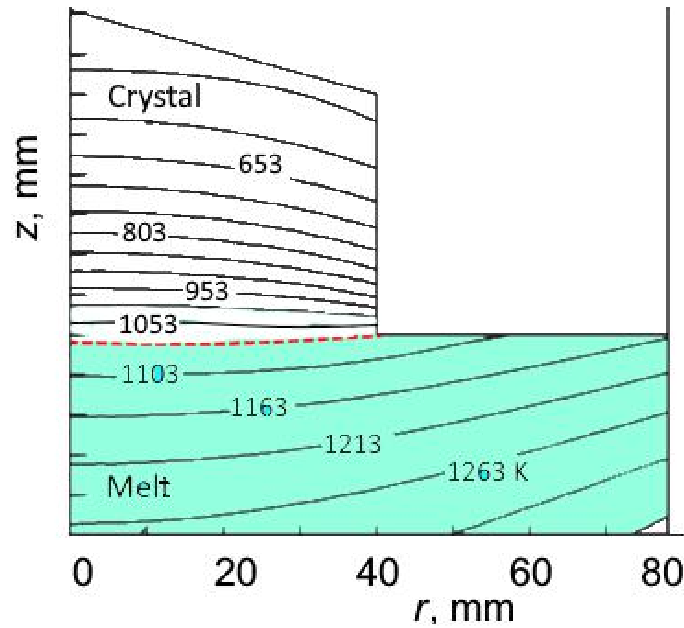

Fig. 1. Typical temperature fields in the "crystal-melt" system during the preparation of a $TlInS_2 < 1$ ат.% Yb $>$ crystal with a diameter of 10 mm at a growth rate of 0.1 mm/h.

Crystal lattice parameters. Partial replacement of indium in $TlInS_2$ with doping ytterbium (Yb) does not change the arrangement of atoms in the supercell and the degree of local deformations of the crystal lattice is insignificant (<1%) (Fig. 2a,b). This is consistent with the structure of $TlInS_2$ ($Tl^{+}In^{3+}S_2^{2-}$), where each In^{3+} cation forms four covalent bonds with four nearest S_2^{2-} anions. In this case, the ionic radius of the doping Yb^{3+} (0.86 Å) is closer to the ionic radius of In^{3+} (0.80 Å) than to the ionic radius of Tl^{+} (1.50 Å).

The geometry of the crystal structure was optimized so that the forces acting on the $TlInS_2$ atoms from the side of the crystal did not exceed 0.1 eV/Å. The obtained results of the optimized lattice parameters $TlInS_2$ and $TlInS_2 <$ Yb $>$ are in good agreement with the experimental data [5, 16]. In DFT calculations, taking into account the contribution of the spin-orbit interaction to the exchange-correlation energy (GGA-PBE) reduces the errors between the calculated and experimental values of the properties, in particular, the band gap (E_g).

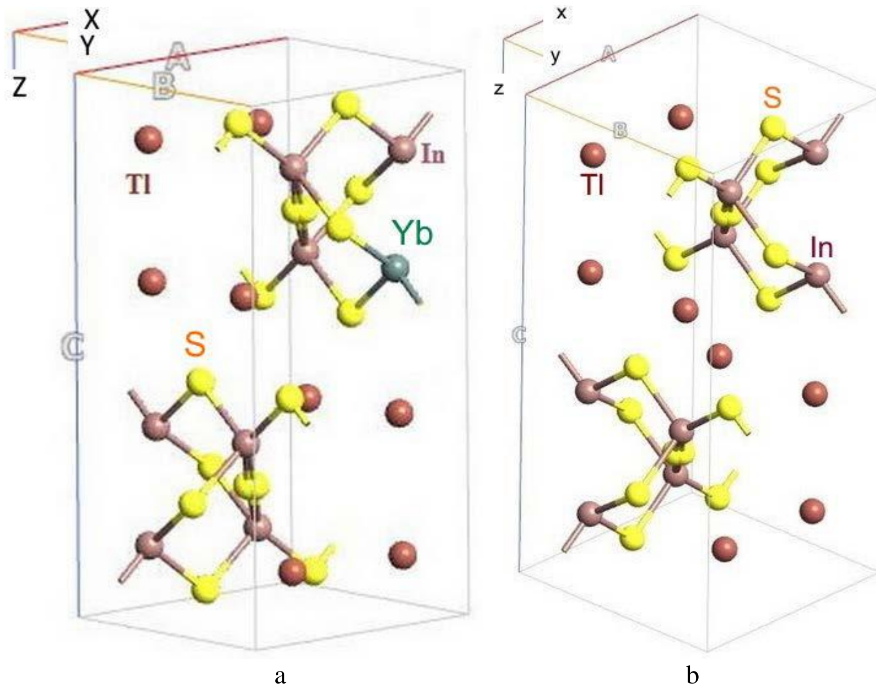

Fig. 2. Atomic structure of the unit cell of the crystal $TlInS_2$ (a) and $TlInS_2 <$ Yb $>$ (b) with a monoclinic system (sp. gr. $C2/c - C_{2h}^6$).

Zone structure. In the band structure of the $TlInS_2$ supercell, the minimum of the valence band and the maximum of the conduction band are located at the Γ point of the Brillouin zone (Fig. 3a,b). $TlInS_2$ has a direct energy band gap $E_g$and is a p-type semiconductor. The results of the DFT calculation of $E_g$without taking into account the effect of spin-orbit coupling and van der Waals interaction are given in Table 1.

It is known that the calculated value of E_g semiconductors is usually less than the experimental data. In order to match and increase the value of E_g, various effects are used and taken into account in the exchange-correlation functional. In particular, taking into account the effect of spin-orbit coupling and van der Waals interaction makes it possible to increase the value of E_g.

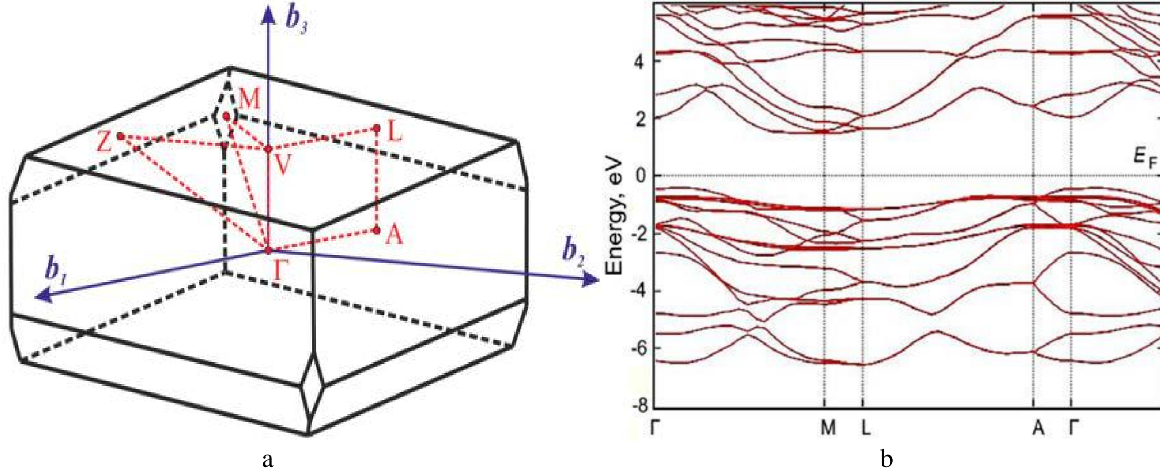

Fig. 3. The first Brillouin zone (a) and the band structure of a $TlInS_2$ crystal with a monoclinic system (sp. gr. $C2/c - C_{2h}^6$) calculated by DFT GGA-PBE 2 × 2 × 2 supercells.

Table 1.

DFT- GGA-PBE calculated and experimental band gaps for 2 × 2 × 2 supercells of $TlInS_2$ and $TlInS_2 < Yb >$ crystals (sp. gr. $C2/c - C_{2h}^6$)

2 × 2 × 2 Supercell	Calculation	Experiment		
	E_g, eV			
	DFT GGA-PBE	77 K	4.2 K [17]	293 K [17]
$TlInS_2$	1.82	2.58	2.516	2.393
$TlInS_2 < Yb >$	1.41	2.53		

Frequency-dependent ac-conductivity. In $TlInS_2$ no significant dispersion of the ε' value is observed in the entire studied frequency range, and its value varies within 9.8–12.2. Ytterbium doping of the $TlInS_2$ crystal leads to a noticeable dielectric dispersion. Thus, with a change in frequency from 5 × 10^4 to 3.5 × 10^7 Hz in the $TlInS_2 < 1$ ат.% Yb $>$ sample, the value of ε' decreased from 11.3 to 5.65, i.e., decreased by a factor of two.

The values of the dielectric loss tangent (tgδ) in the single crystal sample $TlInS_2 < 1$ ат.% Yb $>$ significantly exceeded the values of tgδ in $TlInS_2$.

In the $TlInS_2$ sample, the tg$\delta(f)$ had a monotonically decreasing character, indicating a loss of through conduction. In contrast to $TlInS_2$, in $TlInS_2 < 1$ ат.% Yb $>$, the dependence tg$\delta(f)$ was characterized by the presence of maxima indicating relaxation losses.

On Fig. 4 shows the result of studying the frequency-dependent ac-conductivity of $TlInS_2$ and $TlInS_2 < Yb >$ single crystals at 298 K. In the frequency range 5 × 10^4–10^7 Hz, the ac conductivity of the $TlInS_2$single crystal varied according to the law $\sigma_{ac} \sim f^{0.8}$, and at $f > 10^7$ Hz, the dependence σ_{ac} (f) was superlinear. The dispersion curve σ_{ac} (f) of the $TlInS_2 < 1$ ат.% Yb $>$ sample also had two slopes: $\sigma_{ac} \sim f^{0.8}$ at f = 5 × 10^4–2.4 × 10^7 Hz and $\sigma_{ac} \sim f^2$ at f >2.4 ×10^7 Hz.

Band-type ac-conduction in semiconductors is mostly frequency independent up to 10^10–10^11 Hz. The experimental dependence $\sigma_{ac} \sim f^{0.8}$ observed by us in the $TlInS_2$ and $TlInS_2 < 1$ ат.% Yb $>$ samples indicates that the σ_{ac} conductivity is due to charge carrier hopping between states localized in the band gap. These can be states localized near the edges of allowed bands and/or states localized near the Fermi level [18].

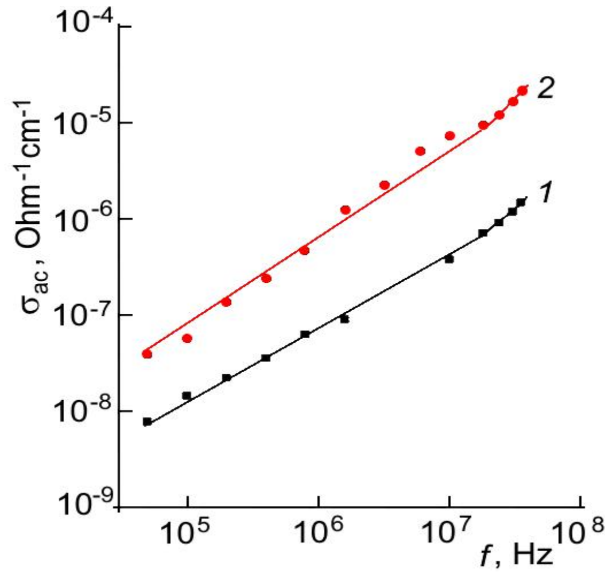

Fig. 4. Frequency-dependent conductivity of single crystals $TlInS_2$ (curve *1*) and $TlInS_2 < Yb >$ (curve *2*) at $T = 298$ K.

In experiments, the conduction over states near the Fermi level usually dominates over the conduction over states near the edges of allowed bands. The law $\sigma_{ac} \sim f^{0.8}$ obtained by us in the samples $TlInS_2$ and $TlInS_2 < 1$ ат.% Yb > indicates a hopping mechanism of charge transfer over states localized in the vicinity of the Fermi level [15, 19]:

$$\sigma_{ac}(f) = \frac{\pi^3}{96} e^2 k_B T N_F^2 a_L^5 f \left[\ln\left(\frac{\nu_{ph}}{f}\right)\right]^4 \quad (5)$$

where e is the electron charge; k_B is the Boltzmann constant; N_F is the density of states near the Fermi level; $a_L = 1/\alpha$ is the localization radius; α is the decay constant of the wave function of a localized charge carrier $\psi \sim e^{-\alpha r}$, ν_{ph} is the phonon frequency.

According to formula (5), ac-conductivity depends on the frequency as $f[\ln(\nu_{ph}/f)]^4$, i.e. at $f \ll \nu_{ph}$, the value of σ_{ac} is proportional to $f^{0.8}$. Using formula (6), the experimentally found values of $\sigma_{ac}(f)$ were used to calculate the density of states at the Fermi level. The calculated N_F value for the $TlInS_2 < 1$ ат.% Yb > single crystal was $N_F = 1.5 \times 10^{19}$ eV^{-1}·cm^{-3}. In the $TlInS_2$ sample, the N_F value was 5.2×10^{18} eV^{-1}·cm^{-3}. Those. doping of the $TlInS_2$ single crystal with ytterbium led to an almost threefold increase in the density of states near the Fermi level. When calculating N_F, the value $a_L = 14$ Å was taken for the localization radius. And the value of ν_{ph} for $TlInS_2$ is taken on the order of 10^{12} Hz [7].

According to the theory of hopping conduction on alternating current, the average hopping distance (R) is determined by the following formula [18]:

$$R = \frac{1}{2\alpha} \ln\left(\frac{\nu_{ph}}{f}\right) \quad (6)$$

In formula (6), the value of f corresponds to the average frequency at which $\sigma_{ac} \sim f^{0.8}$ is observed - the law. The value of R calculated by formula (6) for the single crystal $TlInS_2 < 1$ ат.% Yb > was 80 Å. In the $TlInS_2$ sample, the hopping distance R was found to be 86 Å. These values of R are approximately 6 times higher than the average distance between charge carrier localization centers in $TlInS_2$ and $TlInS_2 < 1$ ат.% Yb > single crystals. The value of R allowed by the formula

$$\tau^{-1} = \nu_{ph} \cdot \exp(-2\alpha R) \quad (7)$$

determine the average hopping time in a single crystal $TlInS_2 < 1$ ат.% Yb >: $\tau = 8.3 \times 10^{-8}$ s. In the $TlInS_2$ sample, τ was found to be 2×10^{-7} s.

According to the formula [18]:

$$\Delta E = \frac{3}{2\pi R^3 \cdot N_F} \quad (8)$$

in $TlInS_2 < 1$ ат.% Yb >, the energy spread of the states localized near the Fermi level was estimated: $\Delta E = 6 \times 10^{-2}$ eV. And according to the formula:

$$N_t = N_F \cdot \Delta E \quad (9)$$

the concentration of deep traps in $TlInS_2 < 1$ ат.% Yb > responsible for ac conductivity was determined: $N_t = 9 \times 10^{17}$ cm^{-3} (in $TlInS_2$ $N_t = 7.3 \times 10^{17}$ cm^{-3}). Doping of the $TlInS_2$ single crystal with ytterbium (1 at.% Yb) led to an increase in the density of states near the Fermi level and to a decrease in the average hopping length and time.

CONCLUSION

Computer modeling of temperature fields in the "crystal-melt" system showed the following. The quality of a single crystal $TlInS_2 < Yb >$ depends on the nature of the temperature fields and the shape of the crystallization front. And the thermal conditions and the shape of the crystallization front, in turn, depend on the crystal diameter and growth rate. The concentration of the Yb (>1 at. %) alloying component along the

"crystal–melt" interface determines the competition between the mechanisms of convection and impurity diffusion. In cases of increasing the concentration of the alloying component Yb, the crystallization rate of the melt $TlInS_2 <$ Yb $>$ is significantly reduced, and the quality of the crystal strongly depends on the temperature fields.

The results of DFT GGA PBE calculations and X-ray phase analysis of the lattice parameters of the single-crystal compound $TlInS_2$ with a monoclinic structure (sp. gr. $C2/c - C_{2h}^6$) are in good agreement with each other and with the known parameters. Without taking into account the effect of spin–orbit coupling and van der Waals interaction, the calculated band gap of the 2 × 2 × 2 $TlInS_2$supercell is E_g= 1.82 eV, which is smaller than the experimental value of E_g. Accounting for these effects and contributions to the exchange-correlation functional makes it possible to increase the value of E_g and agree with the experimental data 2.58 eV at 77 K.

The charge transfer mechanism (hopping transfer mechanism) of $TlInS_2$ and $TlInS_2 < 1$ ат.% Yb $>$ single crystals has been established. In the frequency range $f = 5 \times 10^4$–2.4×10^7 Hz, the ac-conductivity of the $TlInS_2 < 1$ ат.% Yb $>$ single crystal obeyed the regularity $\sigma_{ac} \sim f^{0.8}$. This is characteristic of the hopping mechanism of charge transfer in semiconductors through states localized near the Fermi level. The density of states near the Fermi level is calculated (5.2×10^{18} eV^{-1} cm^{-3} for $TlInS_2$ and 1.5×10^{19} eV^{-1} cm^{-3} for $TlInS_2 < 1$ ат.% Yb $>$), their energy spread (0.14 eV for $TlInS_2$ and 6×10^{-2} eV for $TlInS_2 < 1$ ат.% Yb $>$), average time (2×10^{-7} s for $TlInS_2$and 8.3×10^{-8} s for $TlInS_2 < 1$ ат.% Yb $>$) and hopping distance (86 Å for $TlInS_2$and 80 Å for $TlInS_2 < 1$ ат.% Yb $>$), as well as the concentration of deep traps (7.3×10^{17} cm^{-3} for $TlInS_2$ and 9×10^{17} cm^{-3} for $TlInS_2 < 1$ ат.% Yb $>$) responsible for ac conduction. Thus, doping with ytterbium (1 at.% Yb) of the $TlInS_2$ single crystal makes it possible to control its physical and dielectric properties.

ACKNOWLEDGMENTS

The work has been partially funded by the Science Development Foundation with the President of the Republic of Azerbaijan (EIF) (grant No. EIF-BGM-4-RFTF-1/2017) and the Russian Foundation for Basic Research (RFBR) (project No. Az a2018).

CONFLICT OF INTEREST

The authors declare that they have no conflict of interest

[1] *S.N. Mustafaeva, M.M. Asadov, A.A. Ismailov.* Phys. Solid State. 2009. V. 51. № 11. P. 2269. https://doi.org/10.1134/S1063783409110122]

[2] *K.R. Allakhverdiev, N.D. Akhmed-zade, T.G. Mamedov* // Low Temp. Phys. 2000. V. 26. № 1. P. 56. https://doi.org/10.1063/1.593863

[3] *K.R. Allakhverdiev, T.G. Mammadov, R.A. Suleymanov.* J. Phys.: Condens. Matter.2003. V. 15. P. 1291. https://doi.org/10.1088/0953-8984/15/8/313

[4] *A.F. Qasrawi, N.M. Gasanly.* J. Mater. Sci. 2006. V. 41. P. 3569. https://doi.org/10.1007/s10853-005-5618-0

[5] *W. Henkel, H.D. Hochheimer, C. Carlone.* Phys. Rev. B. 1982. V. 26. P. 3211. https://doi.org/10.1103/PhysRevB.26.3211

[6] *H. Hahn, B. Wellman.* Naturwis. 1967. V. 54. № 2. P. 42. https://doi.org/10.1007/bf00680166

[7] *S.N. Mustafaeva, M.M. Asadov, C.C. Huseynova.* Phys. Solid State. 2009. V. 64. № 6. P. 628.

[8] *B.I. Shklovskii, A.L. Efros.* Electronic Properties of Doped Semiconductors. Springer, Berlin, Heidelberg. 1984. 393 p. ISBN: 978-3-662-02403-4

[9] *M.M. Asadov, S.N. Mustafaeva, S.S. Guseinova.* Phys. Solid State. 2021. V. 63. № 5. P. 797. https://doi.org/10.1134/S1063783421050036]

[10] *J.P. Perdew, K. Burke, M. Ernzerhof.* Phys. Rev. Lett. 1996. V. 77. № 18. P. 3865. https://doi.org/10.1103/physrevlett.77.3865

[11] *H.J. Monkhorst, J.D. Pack.* Phys. Rev. B. 1976. V. 13. № 12. P. 5188. https://doi.org/10.1103/physrevb.13.5188

[12] CGSim Flow Module Theory Manual, STR Inc., Richmond, VA, USA. 2011.

[13] *S.N. Mustafaeva, M.M. Asadov, N.Z. Gasanov.* Inorg. Mater. 2013. V. 49. № 12. P. 1175. https://doi.org/10.1134/S0020168518070099

[14] *S.N. Mustafaeva, M.M. Asadov, S.S. Guseinova.* Phys. Solid State. 2022. V. 64. No 4. P. 428. https://doi.org/10.21883/FTT.2022.04.52182.251

[15] *S.M. Asadov.* J. Phys. Chem. A. 2022. V. 96. № 2. P. 259. http://dx.doi.org/10.1134/S0036024422020029

[16] *S. Kashida, Y. Kobayashi.* +J. Phys.: Condens. Matter. 1999. V. 11. № 4. P. 1027. https://doi.org/10.1088/0953-8984/11/4/010

[17] Semiconductors. Data Handbook, Ed. by O. Madelung. Springer, Berlin, 3rd ed. 2004. ISBN 978-3-642-62332-5.

[18] *N.F. Mott, E.A. Davis.* Electronic Processes in NonCrystalline Materials, 2nd ed. Oxford Univ. Press. New York. 2012. 590 p. ISBN 978-0-19-964533-6.

[19] *M. Pollak.* Philos. Mag. 1971. V. 23. P. 519. http://dx.doi.org/10.1080/14786437108216402